Available online at www.sciencedirect.com

SCIENCE DIRECT®

Journal of Non-Crystalline Solids 352 (2006) 185–188

JOURNAL OF
NON-CRYSTALLINE SOLIDS

www.elsevier.com/locate/jnoncrysol

Letter to the Editor

Making amorphous steel in air by rare earth microalloying

C.Y. Luo [a], Y.H. Zhao [a], X.K. Xi [a], G. Wang [a], D.Q. Zhao [a],
M.X. Pan [a,*], W.H. Wang [a], S.Z. Kou [b]

[a] *Institute of Physics, Chinese Academy of Sciences, Extreme Conditions Laboratory, Beijing 100080, People's Republic of China*
[b] *State Key Laboratory of Gansu Advanced Nonferrous Metal Materials, Lanzhou University of Technology, Lanzhou 730050, People's Republic of China*

Received 24 January 2005; received in revised form 14 November 2005
Available online 20 December 2005

Abstract

Recently great advancement in the fabrication of structural amorphous steels (SASs) with large cross-section sizes has been obtained. One of the remained key problems for the manufacturability and the application of SASs is that their glass-forming ability is very sensitive to the processing environments. Here we present the discovery that the bulk amorphous alloy $Fe_{44}Mn_{11}Cr_{10}Mo_{12}C_{15}B_6Ho_2$ has high oxygen resistance and can be prepared by conventional copper-mold casting method in air atmosphere. Rod-shaped amorphous samples of diameter up to 6 mm at least have been fabricated successfully. This amorphous steel alloy showed high glass-forming ability and good manufacturability. The beneficial effects of the addition of holmium on the glass-forming ability and oxygen resistance during the SAS formation are explored.

PACS: 71.23.Cq; 71.55.Jv; 81.05.−t; 81.05.Zx

Keywords: Amorphous metals; Metallic glasses; Glass formation

1. Introduction

Fe-based amorphous alloys show great potential as engineering materials for structural and functional applications because of their unusual mechanical and physical properties such as high strength and hardness, excellent magnetic properties, and better corrosion resistance, as well as much lower raw material cost [1–6]. Thin ferromagnetic strips, for example, have been commercially available since the 1980s [5]. However, these glasses are fabricated by melt spinning method at rates on the order of 10^6 K/s because of the limit of the glassy forming ability (GFA). The thin strip glasses with a thickness of smaller than 200 μm are impossible to be used as functional and structural materials for engineering uses where the bulk metallic glasses (BMGs) are needed [7]. Thus, Fe-based BMGs have attracted much attention since their discovery, and great efforts have been devoted to this field.

Recently great progress in non-magnetic Fe-base BMGs is a significant increase in glass formability by microalloying with elements of yttrium and erbium. The representative compositions are $(Fe_{44.3}Cr_{10}Mo_{13.8}Mn_{11.2}C_{15.8}B_{5.9})_{98.5}Y_{1.5}$ [8] and $Fe_{48}Cr_{15}Mo_{14}Er_2C_{15}B_6$ [9]. The sample of diameter up to 12 mm has been obtained by conventional copper-mold casting in argon environment. These Fe-based bulk amorphous alloys are called non-ferromagnetic steel alloys or structural amorphous steels (SASs). The SASs exhibit non-ferromagnetism at room temperature, higher hardness and better corrosion resistance. However, the GFA of SASs depends dramatically on oxygen level in the processing environment which can obviously deteriorate their GFA. Therefore, the preparation of the SASs has to be performed in high vacuum or high purity argon atmosphere with very

---

[*] Corresponding author. Tel.: +86 10 82649196; fax: +86 10 82640223.
E-mail address: panmx@aphy.iphy.ac.cn (M.X. Pan).

0022-3093/$ - see front matter © 2005 Elsevier B.V. All rights reserved.
doi:10.1016/j.jnoncrysol.2005.11.013

clean environment. The unfavorable effect of oxygen is a key factor to degrade the manufacturability of the SASs and limits their applications. Our previous work showed that the Zr-based BMGs with a proper amount of yttrium addition can be obtained at low vacuum using low purity components [10]. The yttrium addition method afterward has been successfully applied to enhance the GFA and manufacturability of Fe-, Cu-based alloys [8,10–12]. In this letter we report that a highly processable $Fe_{44}Mn_{11}Cr_{10}Mo_{12}C_{15}B_6Ho_2$ alloy exhibits high GFA and oxygen resistance. It can be easily injected into amorphous rod up to 8 mm diameter at least in argon atmosphere and 6 mm diameter in air atmosphere by conventional copper-mold casting and using commercial-grade raw materials. The present fabrication method can markedly simplify the fabricating process and would be of tremendous benefit for commercialization applications of SASs.

2. Experimental methods

Multi-component master alloys with a composition of $Fe_{44}Mn_{11}Cr_{10}Mo_{12}C_{15}B_6Ho_2$ (at.%) were prepared by arc melting of commercial-grade raw materials (with purities from 99% to 99.5%) in a water-cooled copper crucible under a molten titanium metal gettered argon atmosphere. The resultant master alloys were then remelted in a quartz tube and then injected into a copper-mold without water cooling (the estimated cooling rate is about 10 K/s) to get the rod-shaped samples in argon and air environments. The amorphous nature of the samples was identified by X-ray diffraction (XRD) with Cu K_α radiation, and confirmed by Perkin Elmer Differential Thermal Analyzer-7 (DTA-7) in a flow of purified argon atmosphere (99.999%) with a heating rate of 20 K/min. The oxygen content of the as-cast cylinders was analyzed by using energy disperse spectrometer (EDS).

3. Results

The $Fe_{51}Mn_{10}Mo_{14}Cr_4C_{15}B_6$ bulk amorphous forming alloy was chosen as an initiative composition for our work [13], and the improvement on GFA of the alloy was made by microalloying of different lanthanide (Ln) elements. The experimental results show that the addition of holmium can significantly enhance the GFA of the $Fe_{51}Mn_{10}Mo_{14}Cr_4C_{15}B_6$ alloy. The optimal alloy composition with Ho addition to form large size glassy sample is $Fe_{44}Mn_{11}Cr_{10}Mo_{12}C_{15}B_6Ho_2$, which can be obtained with a diameter of 8 mm at least in argon atmospheres whereas up to a diameter of 6 mm in air atmosphere. Fig. 1 shows the XRD patterns of the cross-section of the as-cast samples of $Fe_{44}Mn_{11}Cr_{10}Mo_{12}C_{15}B_6Ho_2$ alloy prepared in argon and air atmospheres, respectively, clearly illustrating that both the samples exhibit broad diffraction maxima characteristic of glass without obvious crystalline Bragg peaks with the detectable limitation of the XRD. The XRD results indicate both the samples cast in argon and air environments contain uniform amorphous structure, demonstrating that the GFA and manufacturability of the alloy are not significantly deteriorated in air atmosphere. The alloy with Ho microalloying is high inert to manufacturability environment and have high oxygen resistance.

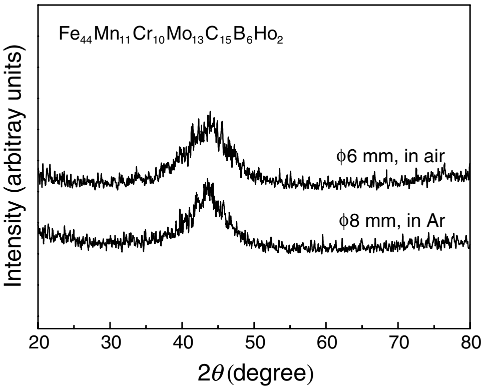

Fig. 1. XRD patterns of $Fe_{44}Mn_{11}Cr_{10}Mo_{12}C_{15}B_6Ho_2$ alloy prepared in air and argon atmospheres.

A camera photo of the $Fe_{44}Mn_{11}Cr_{10}Mo_{12}C_{15}B_6Ho_2$ glassy rods (8 mm and 6 mm in diameter prepared in argon and air atmospheres, respectively) is shown in Fig. 2. The 8-mm-diameter sample prepared in Ar atmosphere has a smooth surface and metallic luster, in contrast, the surface of the sample prepared in air was oxidized obviously, but beneath the oxidized scarfskin it shows a homogenous amorphous structure and a shiny fractured appearance like other Fe-based bulk glassy alloys.

Fig. 3 shows DTA traces obtained from the $Fe_{44}Mn_{11}Cr_{10}Mo_{12}C_{15}B_6Ho_2$ amorphous samples prepared in argon and air atmospheres, respectively with a heating rate of 20 K/min. The two samples exhibit very similar DTA traces: three exothermic crystallization peaks, and same endothermic characteristic of melt peaks at higher temperatures, further confirming the amorphous structure of these

Fig. 2. A camera photo of $Fe_{44}Mn_{11}Cr_{10}Mo_{12}C_{15}B_6Ho_2$ SAS samples prepared in argon (left) and air (right) atmospheres.

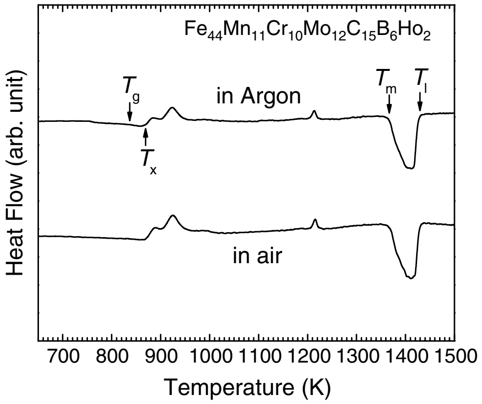

Fig. 3. DTA traces of the $Fe_{44}Mn_{11}Cr_{10}Mo_{12}C_{15}B_6Ho_2$ alloy prepared in air and argon atmospheres.

samples. The values of thermal properties of the glass transition temperature T_g, the onset temperature of the first crystallization event T_x, the melting temperature T_m and the supercooled liquid region ΔT_x ($=T_x - T_g$) of the alloys prepared under two different conditions are listed in Table 1. For the alloy, the high GFA is attained despite a low reduced glass transition temperature T_{rg} ($=T_g/T_m$) [14] of 0.587 and a narrow supercooled liquid region about 30 K. The alloy exhibits a single endothermic peak with small melting range of about 60 K, indicating that the composition of the $Fe_{44}Mn_{11}Cr_{10}Mo_{12}C_{15}B_6Ho_2$ alloy is very close to the eutectic point. The T_{rg} and γ [$\gamma = T_x/(T_g + T_l)$] [15], which are generally used as criterion in evaluating the GFA of an alloy, are almost the same for two samples. Therefore, above results confirm that the preparation of the SASs in air condition does not obviously change the thermal properties, GFA and melting process of the alloy and the GFA of the SAS is highly steady even in oxygen environment.

4. Discussions

The underlying mechanisms of the superior oxygen resistance of the novel SAS are threefold: (1) Ho has larger radii (~0.177 nm) comparing with other elements of the compensation. The Ho addition causes the more optimizing atomic size distributions and increases the complexity of the alloy which limits the solid-state solubility of these elements. Consequently, the packing density and viscous of undercooled liquid are increased and the liquidus temperature is decreased with adequate amount of Ho addition. Thus the stability of supercooled liquid state of the alloy with low atomic diffusivity is enhanced, and then the GFA is also markedly improved. (2) During melting in air, we find that although the alloy does oxidize heavily a uniform oxide film forms and covers the molten alloy which prevents the further contact between air and the molten alloy. (3) From the thermodynamic point of view, Ho has a stronger affinity with the oxygen compared with the other non-lanthanide elements in the alloy. The reaction between Ho and O is thermodynamically favored compared with other oxidation reactions in the alloy. Therefore, in the molten alloy liquid, Ho element is inclined to pervade to surface of the liquid, and reacts with oxygen to form the denser alloy oxide film. This oxide film prohibits the further reaction between alloy liquid and oxygen during melting and casting processes. The EDS analyses of oxygen content in as-cast samples and oxide remained in bottom of quartz tube in air environment are carried out. The results show that there is no obvious difference of oxygen between the two SAS samples prepared in argon and air atmosphere, respectively. However, much high oxygen and Ho contents are found in oxide film compared to that of as-cast samples suggesting that the oxidation behavior of the Fe-based alloy is changed owing to the addition of Ho. The oxide film containing Ho plays a crucial role in the particularly high oxygen resistance of the alloy.

5. Conclusions

The $Fe_{44}Mn_{11}Cr_{10}Mo_{12}C_{15}B_6Ho_2$ SASs with high GFA and oxygen resistance have been synthesized successfully both in argon and air environments using commercial raw materials and copper-mold casting technique. It is apparent that the SAS forming alloy with the addition of rare earth element Ho has good manufacturability in air atmosphere. The present fabrication method can greatly simplify the fabricating process and would be of tremendous benefit for commercialization applications of SASs. The current result demonstrates that the rare earth element microalloying could be very effective in enhancing GFA and manufacturability in the development of new SASs.

Acknowledgements

This work was sponsored by the National Natural Science Foundation of China (Grant No.: 50371098 and 50321101) and the National High Technology Research and Development Program of China (Contract No.: 2001A A320703) and the Key Project of the Beijing Science and Technology Program (Contract No: H02040030320).

Table 1
Thermal properties and rod diameters of the $Fe_{44}Mn_{11}Cr_{10}Mo_{12}C_{15}B_6Ho_2$ SASs prepared under different environments

Sample	Diameter (mm)	T_g (K)	T_x (K)	T_m (K)	T_l (K)	ΔT_x (K)	T_{rg}	γ
$Fe_{44}Mn_{11}Cr_{10}Mo_{13}C_{15}B_6Ho_2$ (in Ar)	Ø8	837	870	1365	1426	33	0.587	0.384
$Fe_{44}Mn_{11}Cr_{10}Mo_{13}C_{15}B_6Ho_2$ (in air)	Ø6	837	868	1367	1428	31	0.586	0.383

References

[1] A. Inoue, T. Zhang, A. Takeuchi, Appl. Phys. Lett. 71 (1997) 464.
[2] A. Inoue, T. Zhang, H. Koshiba, J. Appl. Phys. 83 (1998) 6326.
[3] T.D. Shen, R.B. Schwarz, Acta Mater. 49 (2001) 837.
[4] T. Mizushima, K. Ikarashi, A. Inoue, Mater. Trans., JIM. 40 (1999) 1019.
[5] R. Hasegawa, J. Magn. Magn. Mater. 215&216 (2000) 240.
[6] K. Hashimoto, K. Osada, T. Masumoto, S. Shimodaira, Corros. Sci. 16 (1976) 71.
[7] M. Yagi, I. Endo, I. Otsuka, H. Yamamoto, R. Okuno, H. Koshimoto, A. Shintani, J. Magn. Magn. Mater. 215&216 (2000) 284.
[8] Z.P. Lu, C.T. Liu, J.R. Thompson, W.D. Porter, Phys. Rev. Lett. 92 (2004) 245503.
[9] V. Ponnambalam, S.J. Poon, G.J. Shiflet, J. Mater. Res. 19 (2004) 1320.
[10] Y. Zhang, M.X. Pan, D.Q. Zhao, R.J. Wang, W.H. Wang, Mater. Trans., JIM 41 (2000) 1410.
[11] Z.P. Lu, C.T. Liu, W.D. Porter, Appl. Phys. Lett. 83 (2003) 2581.
[12] D.H. Xu, G. Duan, W.L. Johnson, Phys. Rev. Lett. 92 (2004) 245504.
[13] V. Ponnambalam, S.J. Poona, G.J. Shiflet, V.M. Keppens, R. Taylor, G. Petculescu, Appl. Phys. Lett. 83 (2003) 1131.
[14] D. Turnbull, Contemp. Phys. 10 (1969) 473.
[15] Z.P. Lu, C.T. Liu, Phys. Rev. Lett. 91 (2003) 115505.